FIRST PROOF

AUTHOR'S PROOF

Transport in Porous Media **00**: 000–000, 1992.

Modelling of Flow Pattern in a Shallow Aquifer Affected by Reservoirs

I. Evaluation of the Flow System by Environmental Tracers

EILON M. ADAR, A. S. ISSAR, S. SOREK, and I. GEV
Ben-Gurion University of the Negev, The Jacob Blaustein Institute for Desert Research, Sede Boker Campus 84993, Israel

(Received: 31 August 1989; in final form: 21 February 1991)

Abstract. A process for identifying and quantifying a spatial subsurface flow pattern in a shallow semi-confined aquifer is presented. The conceptual model is aimed at describing the hydraulic effects of surface reservoirs on a shallow semi-confined conducting layer that results in salinization of the top soil. A qualitative study of the relationship between water load in reservoirs, the artesian conducting layer, and water in the top soil was based on chemical and isotopic characteristics. Results indicate limited infiltration from reservoirs into the top soil layers and probably no penetration of water into the conducting layer. Results were then used to establish the regional flow pattern emphasizing the role of surface reservoirs on the build up of artesian pressure in the shallow conducting layer. The flow system was formulated using a compartmental approach in which the unknown parameters are the various sources of recharge and the physical parameters of the aquifer are. A complete mathematical setup and suggested solution for the mathematical algorithm are presented in a second paper.

Key words.

1. Introduction

Up to 60% of the Yizrael Valley was covered by marshes until the beginning of this century, when an intensive deep drainage system kept the brackish groundwater a few meters below the soil surface. As a result, one of the most fertile basins in Israel was increated. However, due to a lack of local fresh water, most of the agricultural activities were nonirrigated dry farming.

Almost 20 years ago, farmers in the valley were offered the use of secondary treated sewage water for irrigation purposes. Due to the microclimate conditions and type of soils involved, this imported water enabled the farmers to move to a double cropping system, namely nonirrigated farming of what during the winter and irrigated cotton and corn during the summer. The supply of treated sewage water is almost constant all the year round. To store the water for irrigation, more than 60 surface reservoirs were constructed in the valley. Most of the reservoirs are situated along the Kishon River and at stream channels in wetlands with deficient natural drainage. Two large reservoirs, Kfar-Baruch and Malle-Kishon (above it), were built on the channel of the Kishon River (Figure 1). The Kfar-Baruch

Key words (1)

Jiezreel Yizrael (2)

paper II (3)

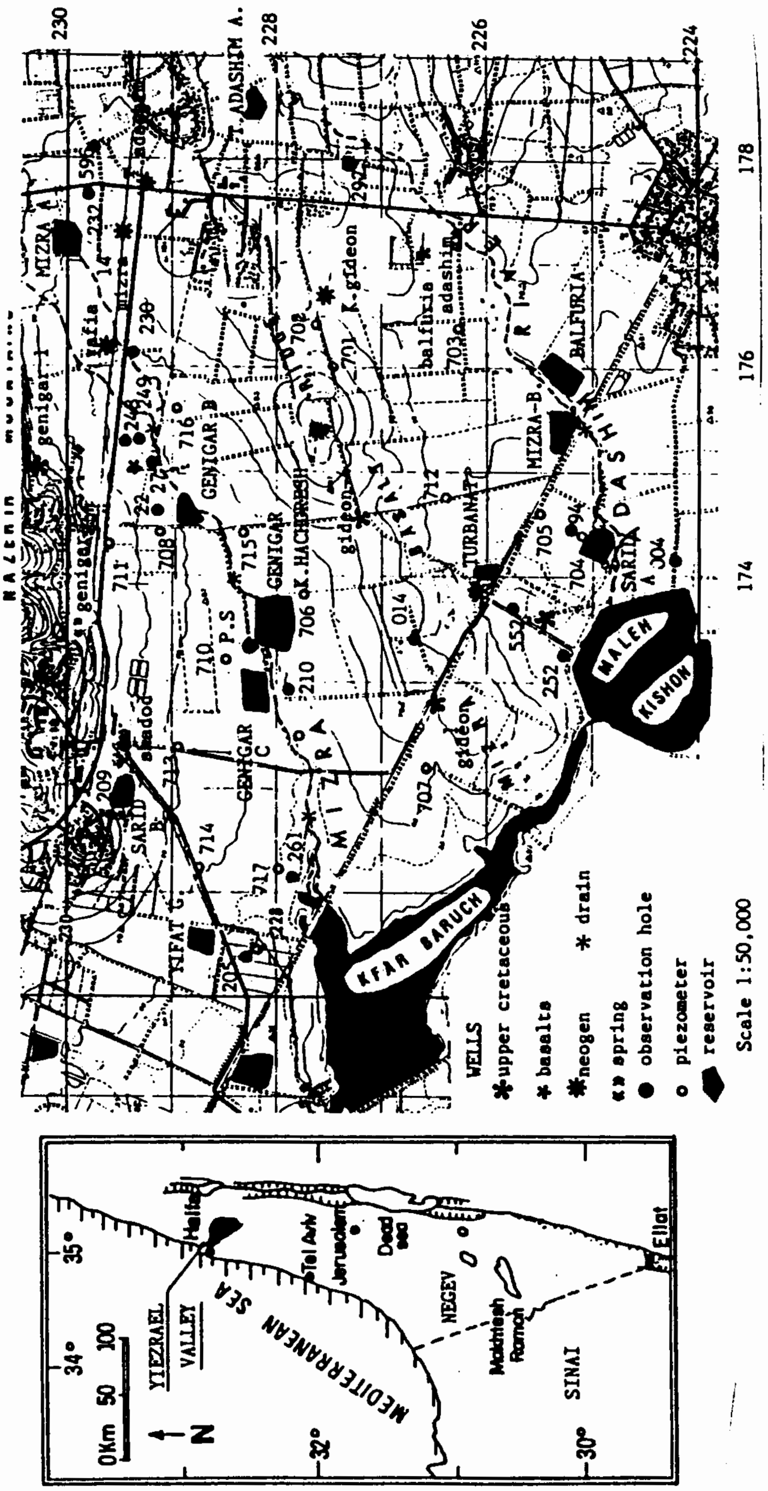
WELLS
upper cretaceous
basalts
neogen
drain
spring
observation hole
piezometer
reservoir
Scale 1:50,000
KFAR BARUCH
MALEH
KISHON
MEDITERRANEAN SEA
YIEZRAEL VALLEY
NEGEV
SINAI
Haifa
Tel Aviv
Jerusalem
Dead sea
Makhtesh Ramon
Eilat
0Km 50 100

reservoir was formed by constructing a dam across the Kishon River. The Malle-Kishon reservoir was constructed with 15 m high embankments above the surface of the Kishon channel, thereby forcing the flow of water in winter to pass around it. This reservoir receives treated sewage water for final oxidation and other treatments before the water is transferred to the Kfar-Baruch reservoir, which also currently serves as a quality-control and operational reservoir for summer irrigation. Water from Kfar-Baruch is pumped into smaller local reservoirs, where it is stored for summer irrigation. A correlation between the location of the reservoirs, high groundwaters, and an increase in soil salinity became evident in the late 1970s. Since then, high groundwater and large saline spots have forced farmers to abandon large cultivated areas in the vicinity of these storage facilities.

Following the clear correlation between reservoir location and the appearance of marshy fields, it was believed that infiltration from reservoirs recharged the top soil, forming a saturated zone in the vicinity of the reservoirs. Therefore, salinization of the top soil was attributed to intensive evaporation from the saturated soils, which increased the accumulation of salts in the top soil. However, an attempt to utilize this unsaturated/saturated hydrological flow model could not provide reasonable realistic results (Revhon and Sinai, 1987). The goal of this model is to estimate aquifer flow parameters and, possibly, to quantify the amount of recharge (upward leakage) into the upper conducting layer. In order to quantify the regional flow pattern and to estimate the flow parameters, we made use of environmental tracers in a form similar to that suggested by Adar and Neuman (1988) and Adar *et al.* (1988).

2. Research Area

The study of the hydrologic system in which surface reservoirs encourage the appearance of saline marshy area was focused on two sub-basins: the Mizra and Adashim basins above Kfar-Baruch, and the Malle-Kishon reservoirs. These basins are separated by a topographic ridge consisting of Neogene basalts which separates the western Yizrael Valley into a low and upper part. The ridge rises from 26 to 30 m at the center of the valley and from 40 to 60 m near the margins. It is important to notice, however, that Kfar-Baruch reservoir was built just below this ridge, and the Malle-Kishon reservoir just above it. In Figure 1, the layout of the reservoirs, stream channels, deep wells, and observation wells are depicted. Thirteen shallow observation wells, up to 6 m below the surface, with 4 to 5 m perforated tubes, and 17, 11 to 12 m deep piezometers were drilled in this phase of the research. Most of the deep piezometers reached a thin semi-confined conducting layer against which perforated tubes were installed. Hydraulic heads were measured monthly in all reservoirs, boreholes, and piezometers in the Mizra and Adashim basin. Five sets of water samples were also taken for chemical and isotopic analysis during 1987–1988.

The hydrogeological structure of the upper alluvial beds in the valley can be observed from information obtained from 11 boreholes and from the 17 new

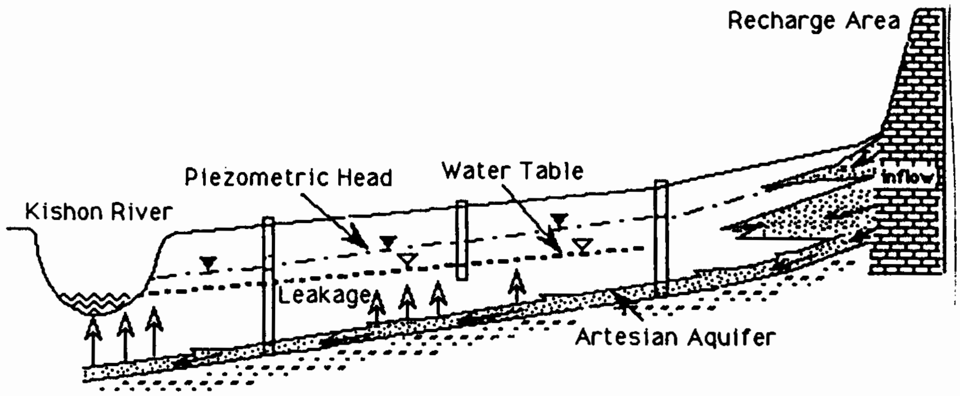

Fig. 2. Schematic pattern of the hydrogeological structure across the research area.

piezometers. The top soil consists of heavily compacted soil, to a depth of 2 to 4 m, and is rich in clay. It covers 3 to 6 m of reddish clay soil containing some thin layers of pockets of gravels. Underneath the clay there is a thin conducting layer, consisting of mixed sand and gravels, overlain by heavy gray marls. In the north, the research area is bordered by the Nazareth mountains (Figure 1), where the upper alluvium contacts the Cenomenian limestones. Lateral recharge may exist from alluvial fans and also by direct contribution from parched mountain aquifers. In the flow model, a temporal water head along this section is assumed. The boundary to the south follows the Kishon River, which drains the top soil and also probably drains the shallow conducting layer. A temporal head, or measured fluxes, can be assigned to this boundary. Both eastern and western boundaries are parallel to the subsurface stream lines and therefore are treated as no-flow boundaries.

The set-up of the general hydrological pattern is presented in Figure 2. The artesian conducting layer is confined by heavy low-permeable soil. It is, therefore, assumed that this layer is drained upward, with leakage into the covering soil, as well as by seepage into the Kishon river in the lower valley. Heads in production wells, which extract water from Neogene basalt layers (40 to 60 m below the surface), indicate that in the lower sections of the basin, the piezometric head just barely reaches the elevation of the conducting layer. Hence, leakage from the Neogene water-bearing layers is unlikely to recharge the conducting layer.

3. Observation and Results

3.1. SALINITY AND HYDRAULIC HEAD DISTRIBUTION

Most reservoirs were constructed just above the saturated soil layer. Since their floors were compacted with heavy clay, infiltration was assumed to be negligible. However, a correlation between reservoirs and the appearance of saline spots became evident. The spatial pattern of top soil salinity in the Mizra and Adashim

Tr /

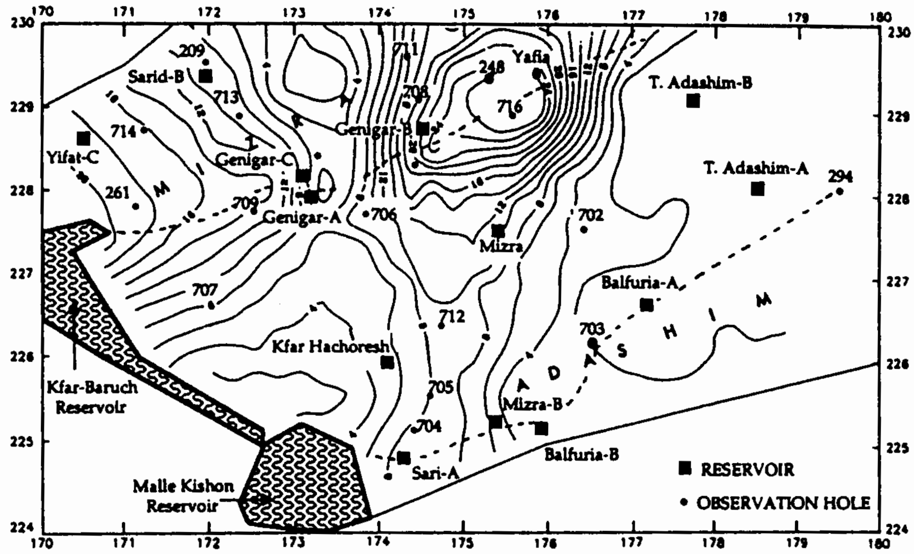

Fig. 3. Salinity distribution in the top soil in mMHO/cm.

basins is described in Figure 3 by the electrical conductivity distribution (in mMHO/cm) of the soil solution. In the Adashim basin, saline spots are found in the vicinity of the sarid-A, Mizra-B and Balfuria reservoirs (6 to 8 mMHO/cm). In the Mizra basin, the level of soil salinity rises to more than 20 mMHO/cm above Genigar-B reservoir and up to 18 mMHO/cm in the vicinity of Kfar-Baruch reservoir. Furthermore, it has been noticed that the piezometric head in the conducting layer is correlated with the soil salinity distribution. This suggest that zones with high salt content in the top soil are related to zones where the piezometric head of the shallow brackish conducting layer is close to the surface.

The distribution of the piezometric head in the Mizra and Adashim basins, illustrated in Figure 4, demonstrates the possibility that reservoirs disrupt the flow in the conducting layer. Piezometric contours show the effect of both on-channel and stream-side reservoirs on groundwater accumulation, namely, a decrease in piezometric gradients above the near reservoirs. A decrease in the piezometric gradient near the reservoirs in February 1988, when all reservoirs were full to capacity is depicted in Figure 4. The piezometric cone near observation well 710 results from heavy pumping from a successful horizontal drainage well. Figure 4 also indicates a significant accumulation in the piezometric head during the winter season, when all reservoirs were completely full. (This situation continued until May, when intensive irrigation began and water levels in reservoirs began to drop.) In general, the piezometric head rose during the winter by more than 2 m at the lower part of the basin (near Kfar-Baruch and Malle-Kishon reservoirs) and at the upstream side of the main storage reservoirs including Sarid-A, Geni-

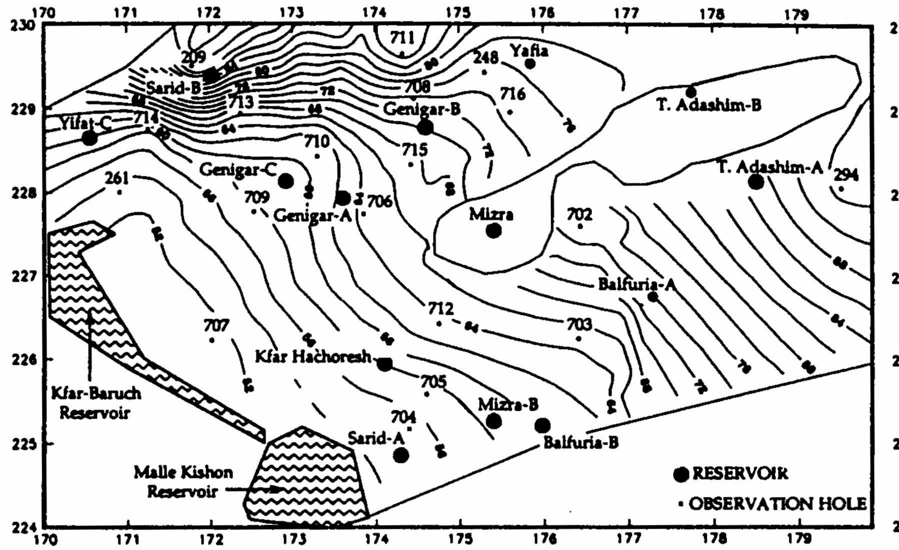

Fig. 4. Piezometric head distribution in February 1988 – reservoirs are at full capacity.

gar-A, B and C. Piezometers located relatively far from the reservoirs show that the head rose by only 0.9 to 1.4 m.

The effect of reservoirs is further demonstrated in Figure 5a, where the longitudinal head profiles for two observations along the Mizra basin are illustrated. High piezometric levels that reach the surface exist at the margin of the basin and in the vicinity of the reservoirs. Moreover, it is clear that when reservoirs are full, the piezometric head over the basin is significantly higher than in periods when water is pumped out of the reservoirs for irrigation (Figure 5b). Piezometer #261 (which is open against the conducting layer) shows a linear correlation with the water head pattern in the Kfar-Baruch reservoir. Figure 5c shows direct relationship between the time-head distribution in Kfar-Baruch reservoir and piezometer #261. It is important to note that the reservoir is not physically connected to the conducting layer. One cannot distinguish, however, between the effect of the rainy season and the piezometric head in reservoirs, since both change during the same period of the year.

Figure 6 shows the water head distribution in the Sarid-A reservoir and in nearby observation holes. Figure 6a demonstrates that water head distribution in the reservoir correlates to the water head pattern in the nearby piezometers. Figure 6b shows piezometric profiles at three time instances in the relation to the water head in Sarid-A reservoir. Close observation and fine head measurements revealed that when Sarid-A reservoir reaches its maximum capacity, the water head in the shallow piezometers (#94B1 and #94B2) exceed that at the deep piezometers (#704). However, when the water head in the reservoir drops, the head in the deep piezometer exceeds that of the 94 shallow series.

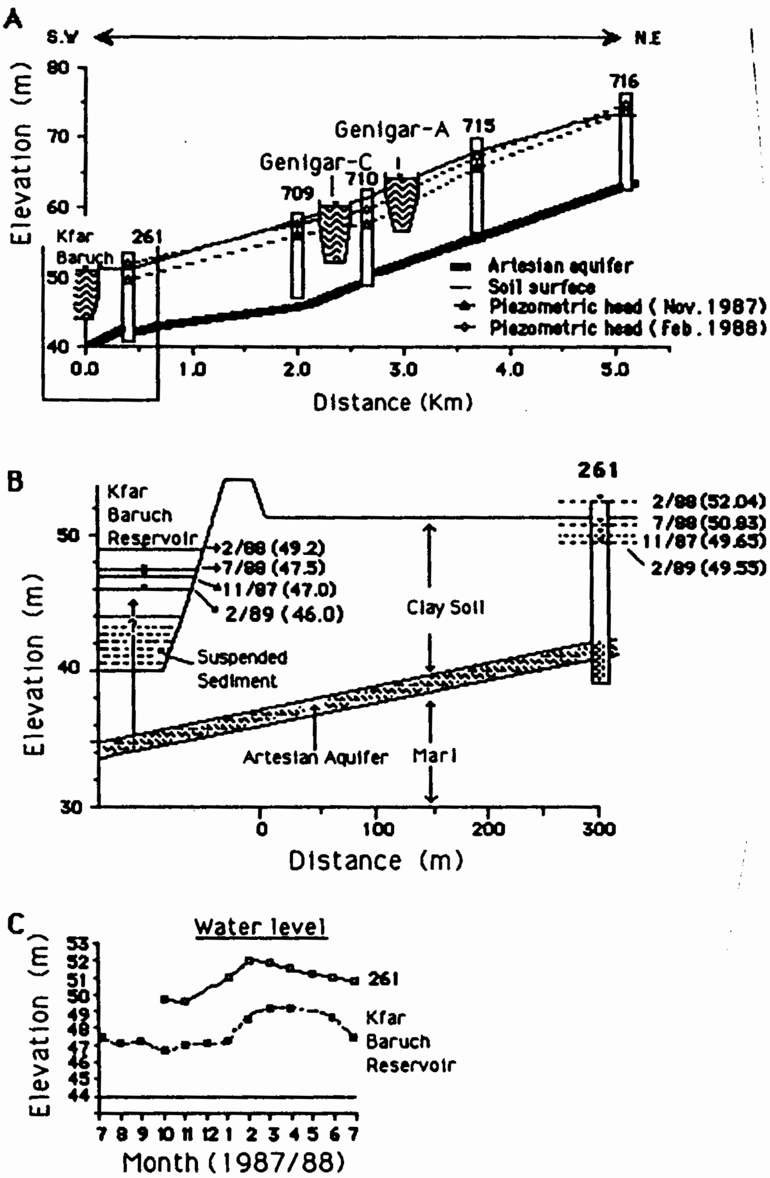

Fig. 5. Piezometric head as related to the water level in reservoirs. (A) Piezometric profiles along the Mizra basins. (B) Relation between the water head in Kfar-Baruch reservoir and piezometer 261. (C) Time distribution fo the piezometric head versus the water level in the Kefar-Baruch reservoir.

3.2. CHEMICAL AND ISOTOPIC CHARACTERISTIC OF WATER IN RESERVOIRS AND IN OBSERVATION WELLS

After a consistent significant correlation between water heads in reservoirs and piezometric heads in the aquifer have been established, ionic and isotopic informa-

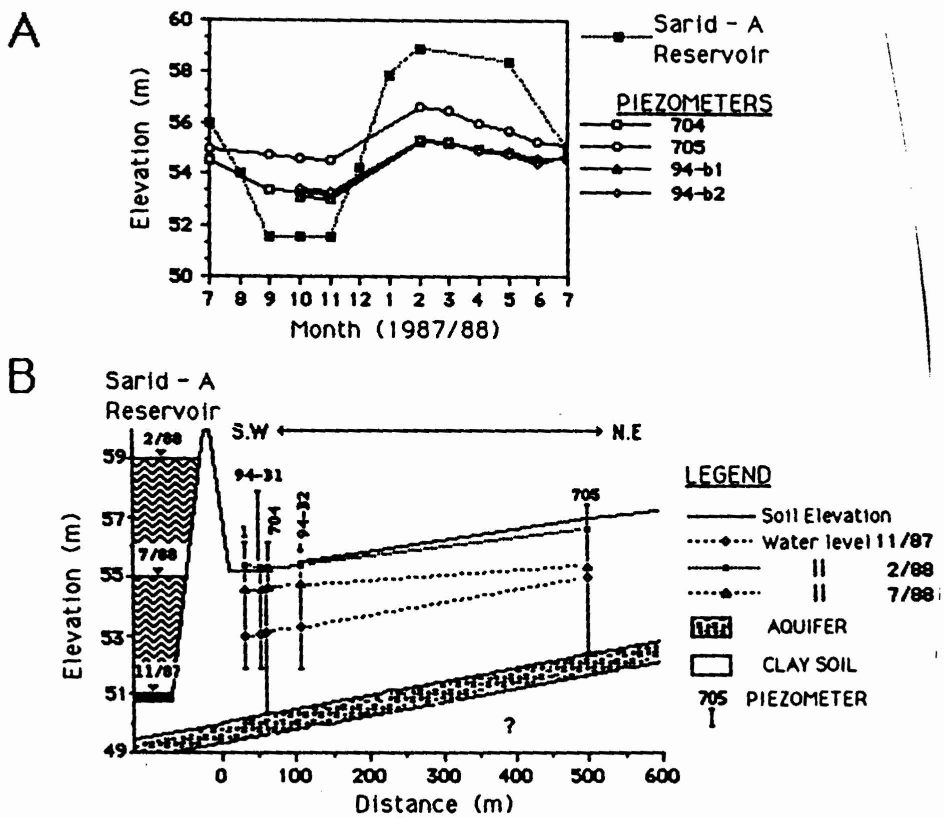

Fig. 6. Distribution of water heads in Sarid-A reservoir and nearby observation holes. (A) Time distribution. (B) Piezometric profiles in three observations.

tion was used to determine the spatial effect of each reservoir on the high piezometric head. The ionic distribution in reservoirs and some nearby piezometers are depicted in Figure 7. The ionic pattern of reservoirs Sarid-A, Genigar-A and Genigar-C differ from the ionic pattern of piezometers located in the vicinity of those reservoirs. The chemical composition of the covering soil in shallow observation holes above the aquifer in the immediate vicinity of a reservoir seems to be only slightly affected by infiltration from the nearby reservoir. This is clearly demonstrated in Figure 7a; where the shallow piezometer #210 and #710, (open against the aquifer and the soil cover) show a chemical mixture between the irrigation water stored in the reservoir (Genigar-A and C) and the water in the aquifer.

Deuterium versus oxygen-18 values for five wells in the vicinity of the four reservoirs is shown in Figure 8. Piezometers #704 and #705 are located 50 and 500 m from Sarid-A reservoir, respectively. Piezometer #209 is 60 m from reservoir Sarid-B, and #708 is located about 100 m north of reservoir Genigar-B. Piezome-

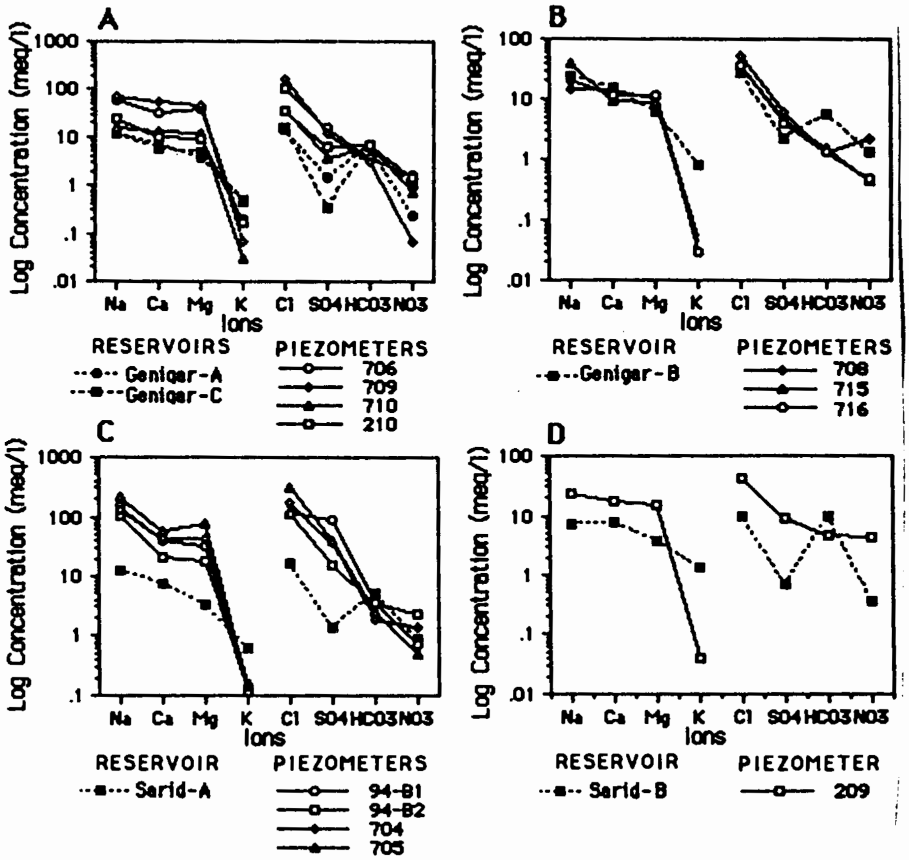

Fig. 7. Chemical composition in reservoirs and nearby piezometers in April 1988.

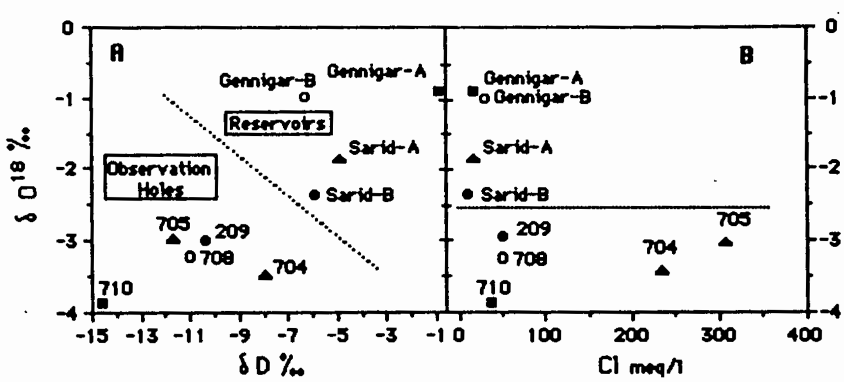

Fig. 8. Oxygen-18 versus deuterium (A) and chlorine (B) in reservoirs and nearby observation holes.

ters 704 and 705 barely touch the conducting layer and probably demonstrate a mixture of water from the artesian aquifer and the bottom of the saturated soil layer. This is further demonstrated in Figure 8b, where the latter piezometers show a significantly higher content of chlorine, dissolved from the soil layer. However, piezometer #710 (located near the pumping station and mostly open against the conducting layer), shows a further depletion in isotopic values. A similar binary diagram for all observation wells in the Mizra and Adashim basins is depicted in Figure 9a. All samples fall below the Mediterranean Meteoric Line, although the water in the reservoirs appear to be the most enriched in heavy isotopes located along an evaporation line. Water samples from observation holes seem to be situated along a mixture line between local rainfall and irrigation water. Isotopic

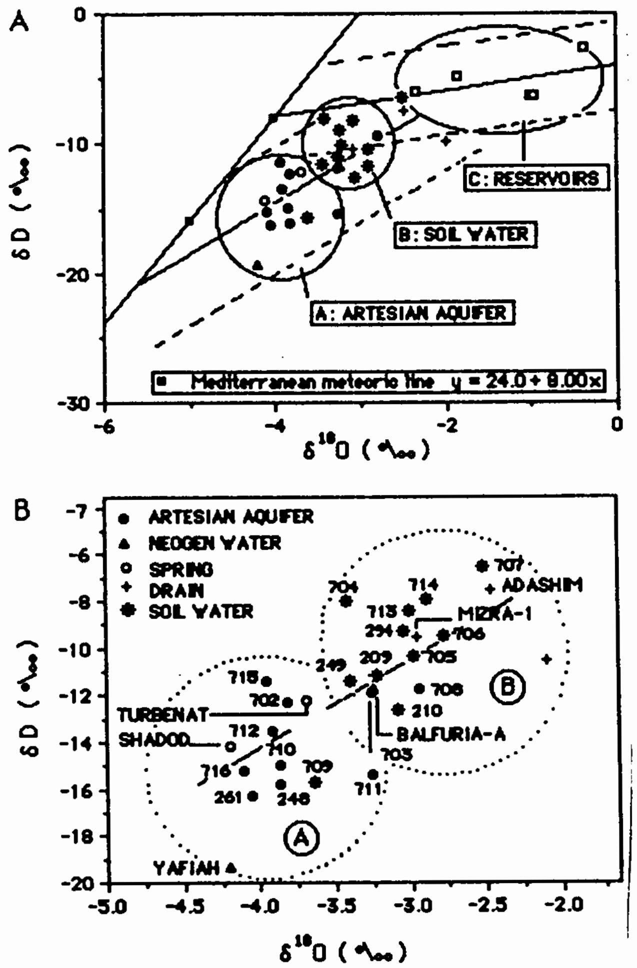

Fig. 9. Deuterium versus oxygen-18 in reservoirs and observation wells (A) and in subclusters from the artesian aquifer and the upper soil cover (B).

distribution among the piezometers distinguish between two subclusters: shallow and deep piezometers. In Figure 9b, the most depleted cluster represents deep piezometers that are opened only against the artesian conducting layer. The upper cluster includes observation holes into the saturated soil cover. This cluster correlates to a mixture line between irrigation water (reservoirs) and water from the conducting layer. In fact, water samples analyzed from shallow drains are among the most enriched samples. In Figure 9b, a well (Balfuria) and a spring (Shadod) may provide water from the Neogene aquifer, 60 to 80 m below the surface. The Balfuria well is situated on the basalt outcrop and its isotopic composition reflects a local (enriched) recharge component. The Yfia well, however, is situated at the foothills of Nazareth Mountains (Figure 1), where the Neogene aquifer is covered by clay soil to a level of 45 m. The water in Shadod spring is probably somewhat enriched in heavy isotopes due to evaporation at the outlet pond.

Deuterium values versus chlorine for both Mizra and Adashim basins are given in Figure 10a and 10b, respectively. In general, reservoir water contains relatively low levels of chlorine. However, this water is enriched in deuterium, as compared with the deep piezometers that are open only against the artesian aquifer. Such deep piezometers in Mizra basin are: #261, #710, #711 p.s. (pumping station), and #702, #703 and #711 in the Adashim basin. Other deep piezometers in which the screen is also open against the saturated soil (just above the aquifer) are still depleted of deuterium, but contain a higher content of chlorine (i.e., piezometers #248 and #709). Shallower piezometers that are more characteristic of saturated soil cover show enriched values of deuterium, as well as higher values of chlorine. Such piezometers are #210, #249, #706, and #707 in the Mizra basin (Figure 10a), and #552, #704, #94B1, and #705 in the Adashim basin (Figure 10b).

Binary diagrams of Na, Ca and SO_4 versus Cl for piezometers in Mizra and Adashim basins are described in Figure 11, which elaborates further on the significant differences in water quality within the conducting layer and the saturated covering soil. Those piezometers which are open against the conducting layer form a cluster depleted in salts. Shallow observation holes, or those that are open mostly against the covering soil layers, demonstrate a high content of dissolved salts. In between the two major clusters, one may find piezometers that extract water from both water bearing layers. The measured amount of isotopes and dissolved ions suggest that the water extracted for laboratory analyses is indicative of the saturated soil cover, although piezometers #709, #713, and #714 represent the water head of the artesian layer. Therefore, one may conclude that water quality is uniformly distributed within the conducting layer, with a slight increase in salinity towards the outlet near the Kishon river.

Chemical and isotopic analyses demonstrated the sensitivity of the hydrochemical data to proper sampling and to the physical setup of the observation wells. It should be noted, that it is quite difficult to identify the chemical and isotopic characteristics of the water for a thin aquifer. This being due to possible mixing with water from the above saturated soil cover unit. Hence, a multi-variable

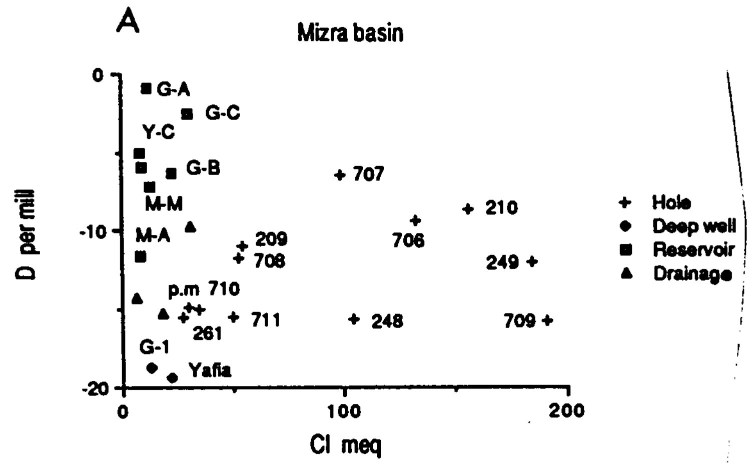

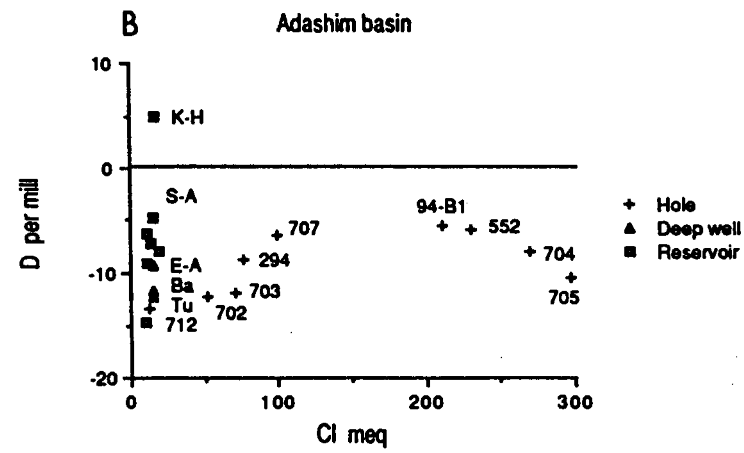

Fig. 10. Deuterium versus chlorine in observation holes and reservoirs in Mizra basin (A) and Adashim basin (B).

analysis was then used to classify the group of piezometers and to assess the relationship between the piezometers and the reservoirs. Electrical conductivity, and the value of eight ions, oxygen-18, and deuterium were used in a statistical cluster analysis using the Ward Method (Everrit, 1980). The above-mentioned elements were used to calculate Squared Euclidean distances to combine a matrix of distances of similarities between observation holes. Results are presented in a dendogram showing the hierarchical clustering relationship among the clusters formed, and also the rescaled distances between 0 to 25, in which clusters and individual observations merge into a single cluster.

Figure 12a presents the dendogram for the Mizra basin. This dendogram indicates five major water types: Group A is a combination of fresh water samples obtained from the upper basin. Water from the pumping station and a nearby

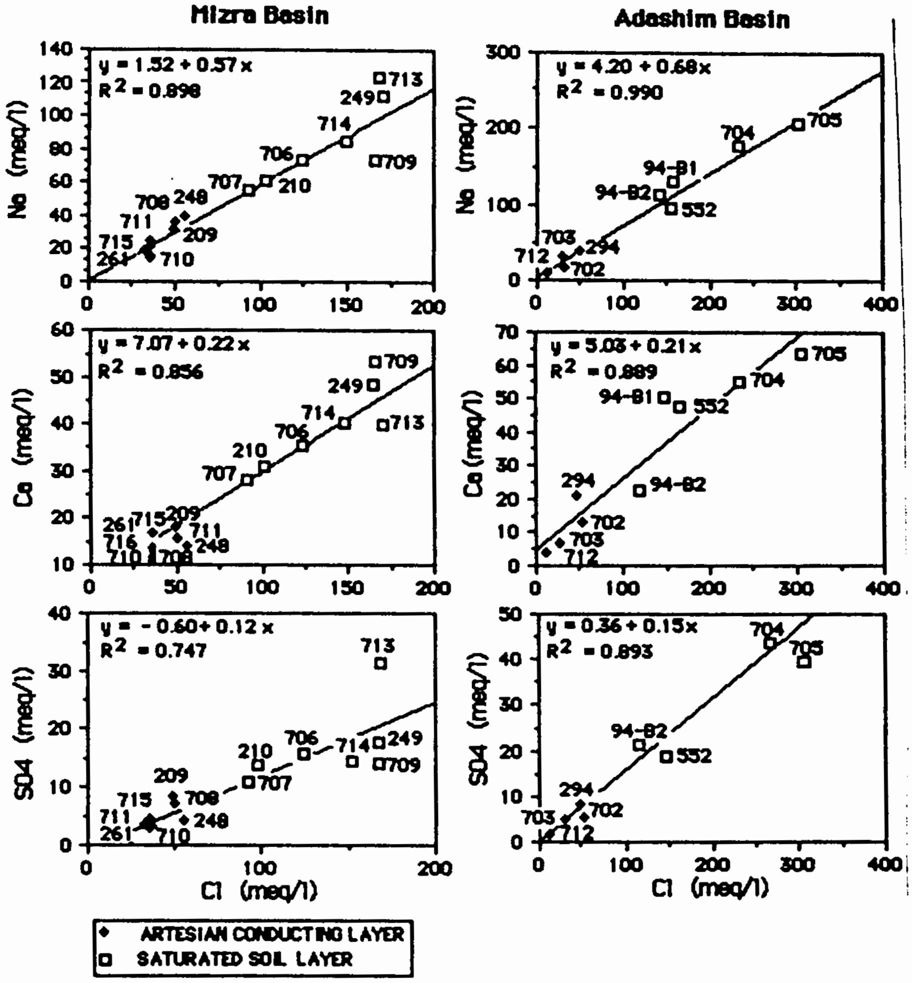

Fig. 11. Binary diagrams of Na, Ca and SO_4 versus Cl.

piezometer #710 are exceptional indicating either the effect of pumping from the conducting layer, or the attraction of fresh water from the margins of the valley. Group B consists of reservoirs that store water from Kfar-Baruch and water from the conducting layer along Mizra river. Group C is a combination of piezometers in the vicinity of the Genigar-C reservoir, except for piezometer #209 which is located near Sarid-B (see Figure 1). Group D represents reservoirs in which water from Kfar-Baruch is mixed with local sewage water. Shadod spring, located near Sarid-B is probably contaminated by this type of water. Group E is distinctly different from other groups, consisting of observation holes that pump water from both the conducting layer and the saturated soil cover. The last two piezometers in cluster E have higher salinity levels and are probably more 'contaminated' by top soil water than other observation holes.

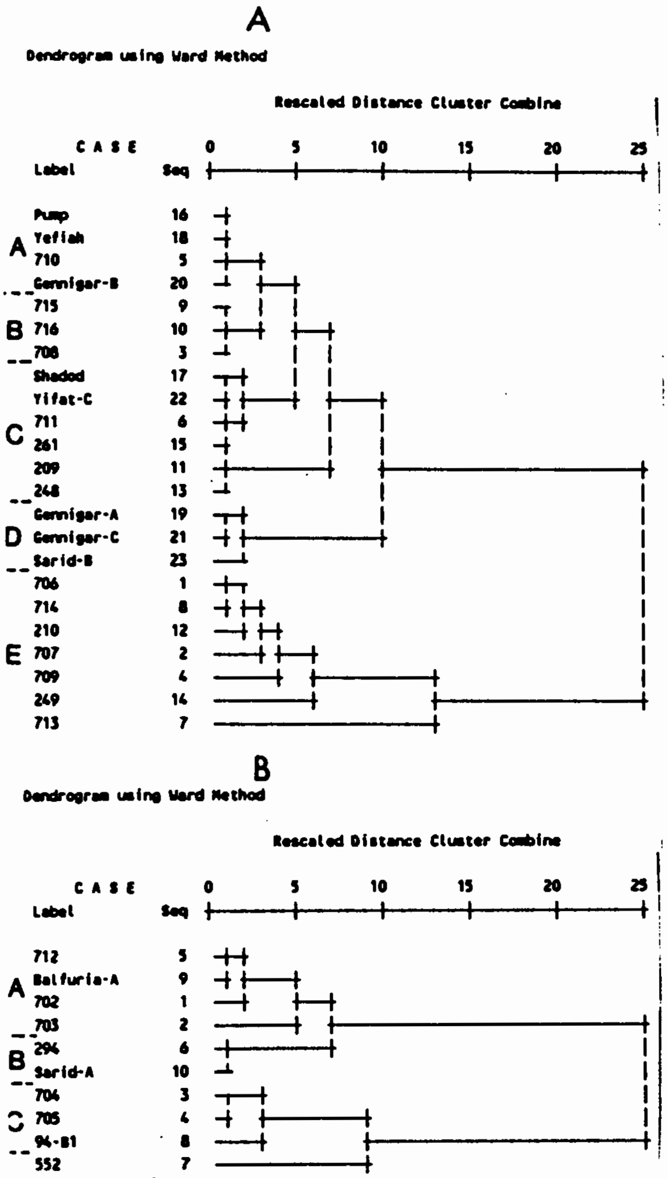

Fig. 12. Dendograms showing clusters of piezometers based on eight ions, electrical conductivity, ^{18}O, and D. (A) Dendogram for Mizra basin. (B) Dendogram for Adashim basin.

Figure 12b shows a dendogram of cluster analysis for the Adashim basin. Group A consists of wells and springs along the Miocene Mizra basalt ridge (Figure 1). This water is of the best quality in the valley, probably originating from local recharge through the weathered basalts or the Neogene deposits. Group B is closely related to Group A as regards the source of recharge, but the piezometers represent more of the saturated soil water than the artesian conducting unit. The Adashim spring is not part of any of the other sources, but is related to the above-mentioned groups. Group C (piezometer #703 and the discharge at the Adashim channel) represent water in the conducting layer along the lower basin. All reservoirs are clustered in a unique group (Group D), which seems to be closely related to Group C. Group E consists of observation wells that extract water from the saturated soil cover in the lower Adashim basin. It is important to note, however, that these samples are totally different and are not related to any of the other groups.

4. The Effect of Reservoirs on the Subsurface Flow System

Isotopic information suggests that the conducting layer is not affected by a mass of water infiltrating from the reservoirs. The conducting layer is probably recharged from the nearby Nazareth mountains and over the Neogene deposits. Just above the aquifer, the isotopic ratio remains depleted as in the aquifer, but the salt content increases immediately. Closer to the soil surface, both the salinity and the ratio of heavy isotopes increase, due to a mixing with evaporated water originating near the surface.

From the piezometric head distribution of the artesian conducting layer and the isotopic and chemical observations, we conclude that the heavy clay soil covers a semi-confined aquifer, and it leaks upward into the covering soil layer because of high artesian pressure. Water from reservoirs do not leak into the artesian layer and infiltration into the soil cover is probably limited to the vicinity of the reservoirs. However, reservoirs which were built over the natural outlet (seepage zone) of the soil water may form hydrostatic barrier that attenuates the natural horizontal flow towards the Kishon River. As a result, additional artesian pressure is built-up within the semi-confined aquifer, increasing the upward leakage into the soil cover. Leakage from below, excess water from irrigation and rainfall, and a disturbed horizontal drainage system force the water to accumulate within the soil cover. The combination of heavy clay soil, a high water table close to the surface, and hot dry weather accelerates the soil water evaporation and, hence, the accumulation of salts in the top layers.

This conceptual model is further examined by a series of eight piezometers close to Kfar-Baruch reservoir. The piezometers were drilled to various depths in one of the most saline fields in the Mizra basin. Detailed stratigraphy revealed that the semi-confined conducting layer is 0.80 to 1.00 m thick, located 9.5 m below the surface. A schematic map showing the location of the observation wells and a table with technical details is given in Figure 13a. Three piezometers: #261, #261/7 and #717 represent the true artesian head of the aquifer. The rest describe the head at various depths in the saturated soil cover. The differences in piezometric heads between shallow and deep piezometers is illustated in Figure 13b. The vertical head gradient is approximately 20 cm along a 5 m interval within the saturated soil. The distribution of chlorine and oxygen-18 along the vertical profile is illustrated in Figure 13c. This figure demonstrates that, except for 261/7, the salinity of the soil

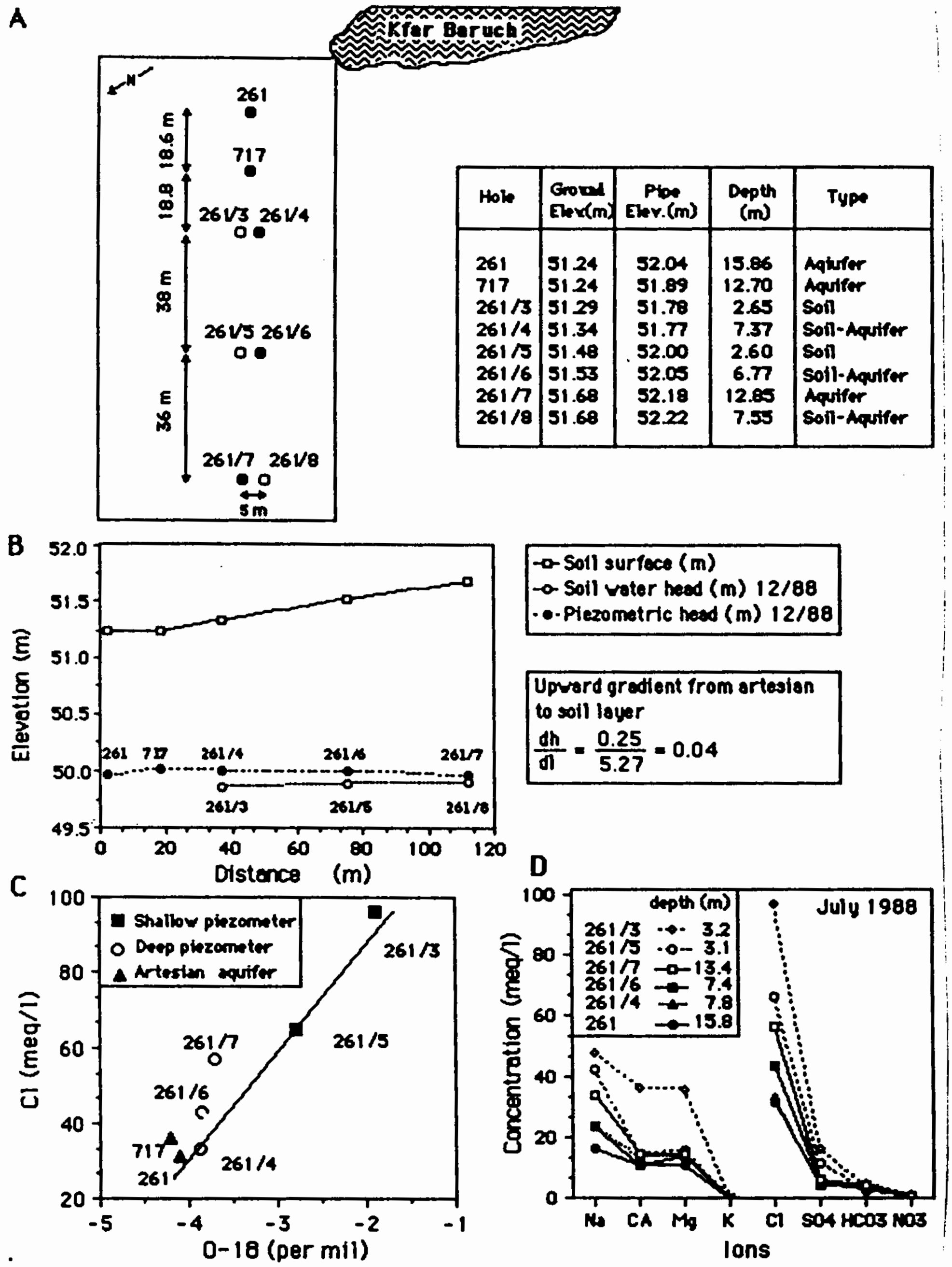

Hole	Ground Elev.(m)	Pipe Elev.(m)	Depth (m)	Type
261	51.24	52.04	15.86	Aquifer
717	51.24	51.89	12.70	Aquifer
261/3	51.29	51.78	2.65	Soil
261/4	51.34	51.77	7.37	Soil-Aquifer
261/5	51.48	52.00	2.60	Soil
261/6	51.53	52.05	6.77	Soil-Aquifer
261/7	51.68	52.18	12.85	Aquifer
261/8	51.68	52.22	7.55	Soil-Aquifer

Fig. 13. Chemical, isotopic and piezometric characteristics in the artesian conducting layer and in the overlain covering soil. (A) Layout of observation wells and technical details. (B) Comparison of water heads within the artesian and soil layers. (C) Chlorine versus oxygen-18. (D) Major ion distribution.

water decreases with depth. Also, the shallow water is enriched with the heavy oxygen isotope. The linear correlation between chlorine and oxygen-18 along the vertical profile, with depleted oxygen at the bottom of the covering soil layer, precludes the possibility of deep percolation from the top soil.

One may suggest hypothesize of a hydrochemical system in which the level of dissolved chlorine is diminished. However, we are not aware of any natural system that can cause a depletion of oxygen-18 in isotopically-enriched infiltrated water. Figure 13d illustrates the distribution of the major anions and cations along the saturated soil profile, down to the artesian conducting layer. Figures 13c and 13d suggest that water dissolves salts as it leaks into the soil cover. Therefore, we conclude that there is upward leakage from the artesian conducting layer, plus an elevated capillary fringe forming a hydraulic barrier that prevents deep percolation. Also there is an attenuation in the horizontal flow forcing the accumulation of water near the surface.

Thus far, a qualitative relationship between water in reservoirs, aquifers, and in the top soil has been established, based on chemical, isotopic and hydrogeologic characteristics. Results, suggest a certain flow pattern, were used to formulate a mathematical model.

5. Mathematical Model

The basic concepts upon which the physical model was constructed are discussed in the following. This model simulates a nonsteady flow system in a shallow semi-confined aquifer affected by the water load in the surface reservoirs, as suggested by analyses of hydrochemical and isotopic information. The model is built upon stable isotopes and chemical composition of water in the reservoirs and the subsurface water-bearing layers. For simplification, the aquifer is discretized into homogeneous compartments. Unique values are given to storativity, hydraulic head, various ion concentrations, and isotopic ratios. This approach follows the mixing cell approach suggested by Campana and Simpson (1984). In each cell, concentrations of environmental tracers (ions and isotopes), the hydraulic head, and the volume of pumping are assumed to be measurable and, hence, known.

The schematic flow system affecting the semi-confined artesian layer is illustrated in Figure 14. For example, cell (n) has an influx from cell (i) and an outflux into cell (j). Upward leakage from (n) into the soil cover is expected, due to a semi-previous layer on top of an aquifer with artesian pressure. Although surface reservoirs are believed to be impermeable, we will allow the possibility of downward leakage only in cells where the head in the reservoir (h_R) is higher than the artesian head (h_n). Hence, for a fluid of constant density, the mass balance for the (n)th compartment ($n = 1, 2, \ldots, N$) is expressed by:

$$\sum_{i=1}^{I(n)} q_{in} - \sum_{j=1}^{J(n)} q_{nj} - (1 - \lambda_n) q_{nR} + \lambda_n q_{Rn} + Q_{bn} + Q_n - W_n = \frac{\mathrm{d}(\phi_n V_n)}{\mathrm{d}t} \qquad (1)$$

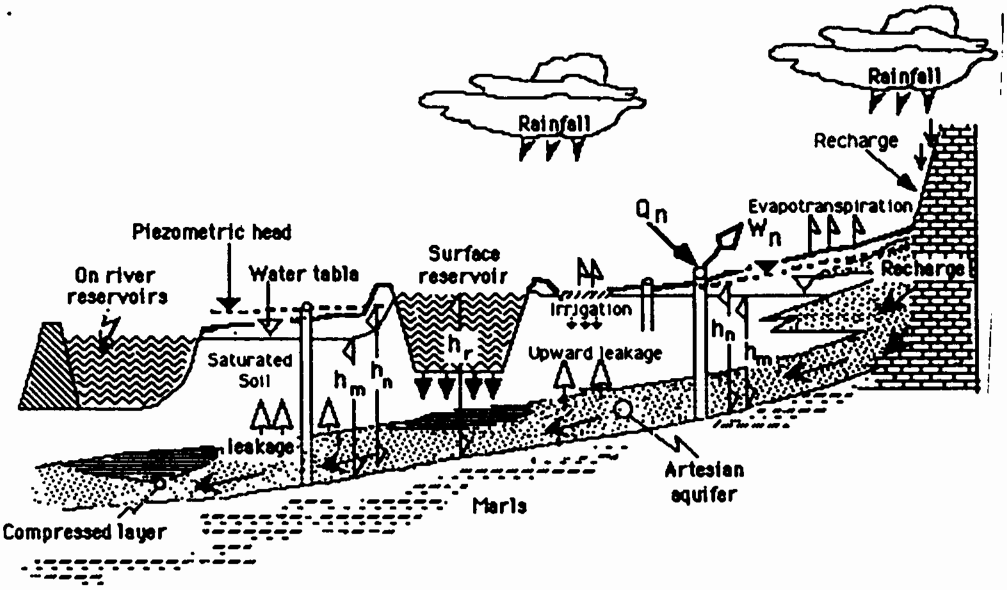

Fig. 14. Schematic flow pattern illustrating flow components associated with symbols for cells and dissolved constituents, as appearing in the mass balance expressions.

where $I_{(n)}$ and $J_{(n)}$ denote the number of compartments from which flow enters (n) and leaves, respectively, q_{in} and q_{jn}, denoting the volumetric fluxes from compartment (i) into (n) and from (n) into the (j)th one, respectively. q_{nR} and q_{Rn} are leakage fluxes from the (n)th compartment into the soil cover and from the surface reservoir into cell (n), respectively. Q_n and W_n denote other fluid sources and sinks in the (n)th compartment, respectively. V_n and F_n denote the volume and porosity of cell (n). It is possible that influx from a lower aquifer, Q_{bn}, may occur along cracks and fissures in the massive marl layers. The coefficient, I_n, conditions the direction of leakage through the top boundary. It is defined by

$$I_n = \begin{cases} 0; & h_n \geq h_R \\ 1; & h_n \leq h_R \end{cases} \tag{2}$$

where h_n and h_R are the head in cell (n) and in the reservoir (R) above it.

According to the water balance expression, each flow component across the permeable boundaries of (n) is associated with a dissolved constituent. Tracers such as stable isotopes of oxygen and hydrogen (O-18 and deuterium), some ion elements (such as chlorine) and dissolved substances or minerals can be used as conservative elements. We also assume that the concentration of various dissolved components governing the transport through the aquifer is dominated by advective processes. Hence, chemical reactions, dissolution or precipitation of substances, and dispersion terms, do not appear in the mass balance expressions of the effluents.

Applying the mixing cell approach, the mass balance equation for the $(k)[k = 1, 2, \ldots, K]$ substance (C_{nk}) in cell (n) is expressed by

$$C_{bk}Q_{bn} + \tilde{C}_{nk}Q_n - C_{nk}\left[W_n + \sum_{j=1}^{J(n)} q_{nj} + (1 - \lambda_n)q_{nR}\right] + \lambda_n C_{Rnk}q_{Rn} + \sum_{i=1}^{I(n)} C_{ink}q_{in} = \frac{d(C_{nk}\phi_n V_n)}{dt}. \quad (3)$$

$\tilde{C}_{nk}$ denotes the concentration being injected into (n) with source flux Q_n. C_{Rnk} denotes the concentration of the (k)thJJYspecien reservoir R, and C_{ink} is the concentration carried with flux q_{in} from cell (i) into (n). The right-hand side of Equation (3) expresses the change in the mass of constituent (k) within (n) during the time step dt. Each cell is associated with $(K + 1)$ balance equations (one water balance equation and K equations for each tracer). If there are (n) cells, there might be up to $N^*(K + 1)$ equations for the entire flow domain.

To evaluate the nonsteady flow system, one first estimates the unknowns associated with each cell. The unknowns are inflows (recharge) and fluxes across permeable boundaries. For internal fluxes, however, where the hydraulic heads are known on both sides of the cell boundary, one may use Darcy's type of expression to estimate conductances at the flow boundaries. Hence, internal fluxes such as q_{in} and q_{Rn} can be replaced by the following expressions.

$$q_{in} = T^*_{in}h_{in} \quad (4.1)$$

and

$$q_{Rn} = b^*_{Rn}h_{Rn}, \quad (4.2)$$

where T^* and b^* are conductances across vertical and horizontal boundaries, respectively. These aquifer parameters are equivalent to transmissivity and vertical hydraulic conductivity used in the simulation of flow in a continuum approach in a manner suggested by Adar and Sorek (1989). The solution for fluxes in such a system is based on Adar and Neuman (1988). A comprehensive description of the mathematical solution to the above-mentioned system is discussed in the following paper (Sorek *et al.* 1992).

6. Conclusion

Environmental isotopes and hydrochemical data from various water sources revealed the effect of on-channel and surface reservoirs on the build up of pressure in a shallow semi-confined aquifer. It has been demonstrated that limited infiltration from reservoirs might contribute water to the water table aquifer in the soil cover layer at the vicinity of the reservoirs. No indications were found, however, for such an effect in the conducting layer. The build up of a high water table in the soil cover is attributed to a disturbance to horizontal drainage and to the upward leakage from the thin artesian aquifer. The leakage is accelerated by an increase in the artesian pressure caused by the reservoirs. Reservoirs were found to be a major cause that significantly decreased the natural horizontal flow towards the draining (Kishon) river. Furthermore, major reservoirs such as Kfar-Baruch and Male-Kishon were found to block the natural outlet of the horizontal drainage from Mizra and Adashim basins, respectively. Hence, artesian pressure is increased in the conducting layer. Such a hydrological barrier is further explained by hydrostatic pressure or even by a slight deformation and compaction of the thin conducting layer, as illustrated in Figure 14. The fact that a cluster of two or three reservoirs was constructed along a natural subsurface flow path further stressed the shallow horizontal drainage system. As a result, additional artesian pressure is built within the semi-confined aquifer, increasing the upward leakage into the soil cover. Leakage from below with elevated capillary fringe, excess water from irrigation and rainfall and disturbed horizontal drainage system force the water to accumulate within the soil cover. The combination of heavy clay soil, a high water table close to the surface, and hot, dry weather accelerates soil water evaporation and, hence, the accumulation of salts in the top layers.

The suggested mathematical formulation describes all potential flow paths revealed through the isotopic and chemical analyses. A compartmental discretization relied on results obtained by the statistical cluster analyses. Hydrochemical data was incorporated into a spatial flow model, expressing balances of water and dissolved constituents. A detailed development of the mathematical algorithm relevant to such compartmental flow system is described in a following article (Sorek *et al.* 1992).

References

Adar, E., Neuman, S. P. and Woolhiser, D. A., 1988, Estimation of spatial distribution using environmental isotopes and hydrochemical data. I. Mathematical model and application to synthetic data, *J. Hydrology* 97, 251–277.

Adar, E. and Neuman, S. P., 1988, Estimation of spatial recharge distribution using environmental isotopes and hydrochemical data. II. Application to Aravaipa Valley in southern Arizona, U.S.A., *J. Hydrology* 97, 279–302.

Adar, E. and Sorek, S., 1989, Multi-compartmental modelling for aquifer parameter estimation using natural tracers in non-steady flow, *Adv. in Water Resour.* 12, 84–89.

Campana, M. F. and Simpson, E. S., 1984, Groundwater residence times and discharge rates using discrete-state compartments model and C-14 data, *J. Hydrology* 72, 171–189.

Everrit, B. S., 1980, *Cluster Analysis*, 2nd edn., Heineman Educational, London.

Revhon, Z. and Sinai, G., 1987, Investigation of the effect of water reservoirs on sub-surface hydrology in adjacent fields, Project Report No. 152-539, Technion, Israel (in Hebrew with abstract and summary in English).

Sorek, S., Bear, J. and Karni, Z., 1989, Resistances and compliances of a compartmental model of the carebrovascular system, *Ann. Biomed. Eng.* 17, 1–12.

Sorek, S., Adar, E. and Issar, A., 1992, Modelling of flow pattern in a shallow aquifer affected by reservoirs: II. Method of estimating flow parameters using environmental tracers, *Transport in Porous Media.*